MIT Kavli Institute for Astrophysics and Space Research

Chandra X-Ray Center

MEMORANDUM

January 17, 2007

To:	Dale Graessle, CALDB
From:	Bish K. Ishibashi, SDS
Subject:	Evaluation on the quality of SAOSAC-based MEG/ACIS-S LSFPARM file for unrandomized event datasets
Revision:	0.1
URL:	http://space.mit.edu/CXC/docs/memo_lsf_ma_0.1.ps
File:	/nfs/cxc/h2/bish/CXC SDS/LSFDIR/HO_LSF_HA_meg/memo_lsf_ma_0.1.tex

1 Need for updating unrandomized LSFPARMS files for MEG/ACIS-S configuration

Our analysis on the merged HETG spectra of Capella revealed a problem with the LSFPARMS products for MEG + ACIS-S configuration. In short, based on the finding by Ishibashi et al. (ApJ, 2006, 644, L117), we successfully merged the existing 12 Capella datasets[1] in the rest frame of Capella's primary star Aa. Upon comparison of the observed line spectral data and a corresponding MEG model line profile, it became clear that the model line width at $\lambda \sim 8.42$Å(i.e., hydrogenic Mg XII), generated with the current LSFPARMS products for MEG $\pm 1^{st}$ orders, appeared to be broader by 0.007Å in FWHM (or $0.16''$ in Gaussian σ angle blur) than that of the observed line profile (see Figure 1).

The root of this problem was identified to be of MARX origin.

MARX internal HRMA models were derived by using a set of SAOSAC ray-trace models generated in early 1998[2]. It is determined that MARX internal HRMA models for the inner two shells (HRMA shells 4 & 6) are not so accurately characterized, while models for the outer two shells (shells 1 & 3) are adequately defined. The minute difference in the MARX PSF width has led to require two different instrumental event repositioning blur factors for the inner and outer shell pairs (i.e., HEG and MEG LSF blur factors), though we were not aware of this. Since (1) the same instrumental blur factor was applied for making the LSFPARMS products for HEG and MEG and (2) the instrumental blur factor was *tuned to match the HEG line data*, the LSFPARMS products were produced with the instrumental blur factor only appropriate for the HEG, but not for the MEG. Since MARX's PSF for the inner two shells was too narrow compared to that of the pre-1998 SAOSAC model, the applied instrumental blur factor was too much for the outer two shell models, which led to the excessive model line width in the MEG's LSFPARMS product.

In order to rectify this "MEG" problem, a new set of the LSFPARMS products for MEG+ACIS-S configuration and for TG-unrandomized events are created. The new LSFPARMS products are generated from today's SAOSAC ray-tracing models for the outer two HRMA shells.

[1] Three of 15 HETGS/ACIS-S datasets were excluded from the analysis since they showed an anomalous sign of the secondary star flaring. See Ishibashi et al. (2006) for details.

[2] Note that the SAOSAC model used for MARX predated an update on Shell 6 mirror tilt added in late 1998.

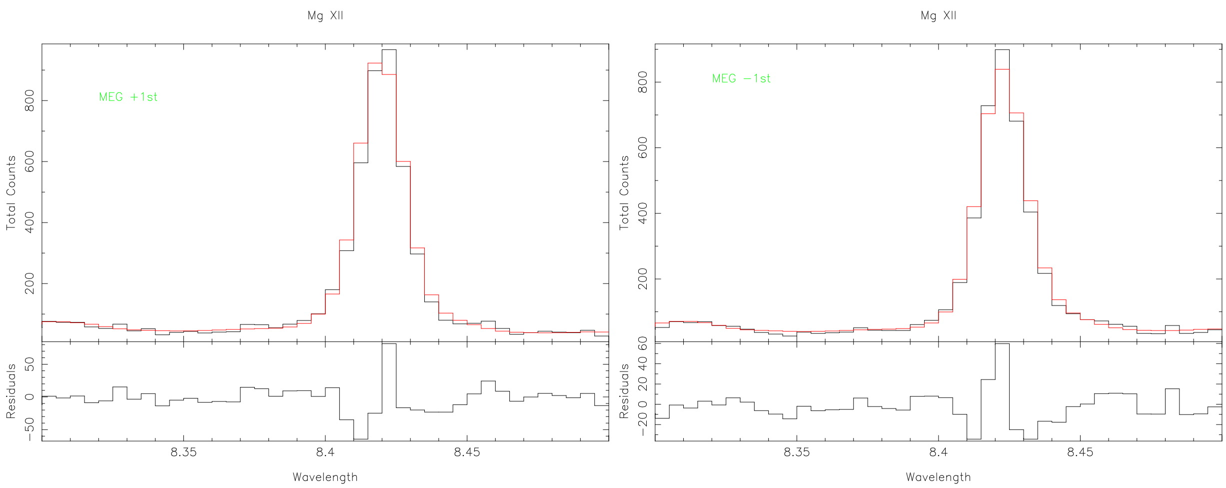

Figure 1: MEG $\pm 1^{st}$ order line spectra of Mg XII for Capella. The solid black line shows the merged data fitted with the thermal APED model (solid red). The difference (residual) between the data and the model is shown in the bottom panel. While their χ^2 statistics are not terribly bad ($\approx 1.7 - 1.8$), it is clear that the model profiles for MEG $\pm 1^{st}$ order are too broad to fit the data profiles.

2 Building new LSFPARMS with SAOSAC

The original procedures for building a LSFPARM file with MARX is described at:

http://space.mit.edu/CXC/LSFX/LSF_valid2.html

Today's SAOSAC (available at the SAO network as in December 2006) was run contiguously nearly over one week CPU time on Solaris machines to generate adequate amount of ray simulations; then the ray files were processed through MARX ver. 4.2.1. The details of SAOSAC/MARX processing will not be illustrated here for brevity.

For rapid development, several parts of IDL parameterization routines are S-Langified for better and faster convergence to optimum fitting parameters through automated processes. In this MEG LSFPARMS processing, the aspect blur factor of $0.03''$ had been adopted (as well as the instrumental blur factor present in the configuration). Note that the aspect blur value was tuned empirically to remove the excessive broadening applied in the earlier MEG products ($\sim 0.12''$).

3 Data products

Two LSFPARM products are developed: MEG $\pm 1^{st}$ orders with HETGS+ACIS-S configuration and without data randomization in TG coordinate. The structure of the new MEG LSFPARMS products are identical to the prior version of the products. There is no new header keyword introduced for the new products.

4 Testing LSFPARM products

4.1 Procedures

Testing of the LSFPARM products are performed with the merged Capella datasets (ObsIDs 57, 1010, 1099, 1100, 1101, 1103, 1235, 1236, 1237, 1318, 2583, and 3674). Three key points for evaluation and testing are

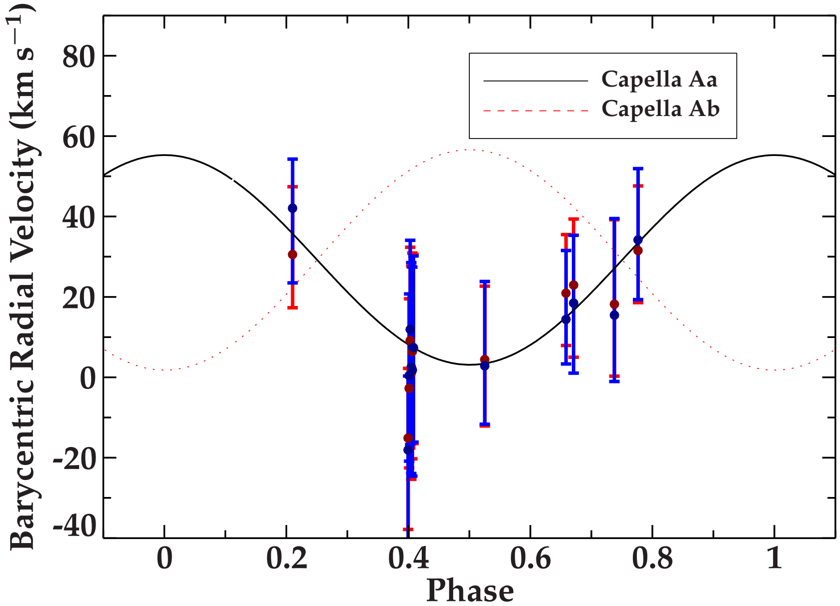

Figure 2: Observed radial motion of Capella vs. orbital phase after barycentric correction (see Ishibashi et al. 2006). The measured radial velocity data with the MEG LSFPARMS products in CALDB are shown in blue; the data points with the new MEG products are shown in red. 3σ error bars are shown in the plot.

the determination of (1) line profile widths, (2) line centroid positions, and (2) enclosed energy fractions (hereafter EEFRAC).

4.2 Evaluation: Chandra Datasets

As described earlier, 12 of 15 Capella datasets were reprocessed with CIAO 3.3 (TG pixel randomization being turned off by default). Before generating each PHA file, each event L1.5 file was corrected for a Doppler motion of Capella's primary star (Capella Aa) so that the merged spectra would emerge with the $10^{6.8}$K emission line features at the rest wavelength. For line centroid analysis, the Doppler correction has been omitted. Corresponding grating RMF products were generated via *mkgrmf* command with the new LSFPARMS files and used as a fitting kernel in *ISIS* for evaluation. Merging of the PHA spectra was also done upon analysis in *ISIS* with the *combine_data* feature. Cash statistics was applied throughout this work.

4.2.1 Line Centroid Analysis

The Doppler velocity measurements of Ishibashi et al. (2006) had been repeated to verify whether the new LSFPARMS products would affect the results. Figure 2 shows that the newly derived velocity measurements are statistically consistent with the earlier measurements (as expected, since the centroid measurements should not be affected by the problem).

4.2.2 Line Profile Analysis

To verify the validity of the new LSFPARMS products, the new MEG LSPARMS products were used to generate a new set of MEG grating RMF and then were used to fit the observed emission lines of Capella. Ideally the fitting results should show no excessive broadening compared to the observed line profiles (c.f., Figure 1).

A thermal X-ray APED model for Capella was used for analysis (with thermal broadening built into the model). Nine bright emission lines – Si XIV (6.1804Å), Si XIII (He-like triplet around 6.7Å), Mg XII (8.4192Å), Mg XI (He-like triplet around 9.2Å), Ne X (12.132Å), Fe XVII (around 17.1Å), O VIII (18.967Å), O VII (He-like triplet around 21.6Å), and N VII (24.779Å)– were selected for testing. Upon fitting, the parameter for line width dv (converted to velocity scale in km s^{-1}) was allowed to vary. Ideally the parameter dv should be ≈ 0 km s^{-1} for thermal APED modeling.

The results of fitting with the APED model is tabulated in Tables 1 and 2. Corresponding figures for line profile fit are shown in Figures 2 and 3. These are not meant to be the best fitting parameters. Upon inspection of Tables 1 and 2, the measured line widths are indeed consistent with 0 km s^{-1} for the most lines. Only the line Ne X shows non-zero broadening on both MEG $\pm 1^{st}$ orders; however the Ne X line is blended with Fe XVII and it is premature to conclude that the model width is too narrow at the wavelength. Note that the error ranges are generally below the MEG energy resolution limit (FWHM $\sim$0.023Å). Furthermore, it is possible that the model requires an additional component, i.e., an addition of the contributed emission from Capella's companion star Ab. The patterns seen in the residual allude that this hypothesis might be feasible. It is to be tested (by someone) in future, as such modeling (notice that Capella Ab is not stationary with respect to Aa) is complicated to make.

4.2.3 Encircled Energy Fraction

To verify the validity of the EEFRAC values in the new MEG LSFPARMS, Capella's MEG $\pm 1^{st}$ order spectra were extracted at four different full extraction widths (not half-width): 3.2×10^{-4} radian (2 CCD pixels), 6.4×10^{-4} radian (4 pixels), 1.28×10^{-3} radian (8 pixels), and 1.92×10^{-3} radian (12 pixels). The third full extraction width is very close to the CIAO default extraction width for `tgextract`.

For each extracted PHA spectrum, the nine individual lines (the same ones used in the section above) were fitted with grating ARF and RMF and then the model fluxes were computed. Ideally, for each emission line, the model fluxes should result in the same value regardless of extraction widths, or plus / minus orders. The measured line fluxes per full extraction widths are tabulated in Table 3. Upon looking at Table 3, it appears that:

- At an extraction width equal to 8 CCD pixels or wider, the measured flux values seem to converge, whereas at a narrower extraction width, the values may weakly depend on the width size.
- There appears to be systematic differences in the measured flux between plus and minus orders.

The first bulletized item may possibly be explained as due to an error in the characterization of line profile (e.g., too much power in the LSFPARMS model at its core; not enough aspect blur, etc...however, see Addendum). It is equally possible that the fitted model may not be adequate and systemically biases the measurements. However, on the second item, the systematic difference is hard to discern. Due to the constraints in the grating model, HETG grating efficiency is practically set to be equal on both plus and minus sides. Likewisely the enclosed energy fraction would remain nearly the same on both sides as well. Having said that, the systemic difference may indicate that the grating efficiencies are not the same on the plus and minus sides. In any case, this seems to be a HETG grating calibration issue rather than the LSFPARMS issue.

Despite some minor differences, the flux measurements show that the line flux values are reproducible at any wide extraction widths (certainly ok at a CIAO default extraction).

4.2.4 Addendum

To see if an additional aspect blur alleviates the differences seen with narrower extraction widths (see Table 3), another set of the LSFPARMS products with an aspect blur of $0.043''$ has been made to test. After repeating the same evaluation, it is noted that the enclosed energy fraction is virtually identical to the LSFPARMS products with an aspect blur factor of $0.03''$. Hence the issue was not resolved by simply broadening the model line profile (and therefore associated grating RMFs).

5 Summary

The validation tests show that the quality of the new LSFPARMS products, made with SAOSAC and MARX, are equally as good as the earlier LSFPARMS products in terms of line centroid and flux measurements. On line width measurements, the new products performs better (i.e., the model profile is not broader than that of the observed data profiles).

Table 1. Capella MEG +1st: thermal APED model.

Element	λ_{lab} (Å)	dv (km/s)	dv 3σ range	χ^2	Comment
Si XIV	6.1804	3.68	0 – 185	1.81	ok
Si XIII	6.6479	71.2	5 – 142	2.69	inadequate line modeling?
Mg XII	8.4192	88.7	0 – 139	1.56	ok
Mg XI	9.1687	38.9	0 – 89.4	6.87	inadequate line modeling?
Ne X	12.1321	99.2	34.3 – 124	1.84	ok (blended lines)
Fe XVII	17.1	0.0	0 – 24.5	2.22	inadequate line modeling?
O VIII	18.9671	0.0	0 – 81.9	1.09	ok
O VII	21.6015	57.6	0 – 149	1.18	ok
N VII	24.7792	60.5	0 – 155	1.06	ok

Table 2. Capella MEG -1st: thermal APED model.

Element	λ_{lab} (Å)	dv (km/s)	dv 3σ range	χ^2	Comment
Si XIV	6.1804	1.85	0 – 329	1.86	ok
Si XIII	6.6479	0.01	0 – 77.1	2.20	inadequate line modeling?
Mg XII	8.4192	124	31.5 – 171	1.49	ok
Mg XI	9.1687	0.51	0 – 51	7.73	inadequate line modeling?
Ne X	12.1321	79.3	22.7 – 115	1.88	ok (blended lines)
Fe XVII	17.1	0.01	0 – 38.7	3.73	inadequate line modeling?
O VIII	18.9671	64.5	0 – 80.6	2.14	inadequate line modeling?
O VII	21.6015	86.7	67 – 163	1.79	ok
N VII	24.7792	34.2	0 – 89.5	1.21	ok

Table 3. Measured Line Fluxes vs. Extraction Widths

	Line Fluxes (10^{-13} erg/s/cm^2) [per Full Extraction Widths (pixels)]							
	plus 1^{st}				minus 1^{st}			
	2 pix	4 pix	8 pix	12 pix	2 pix	4 pix	8 pix	12 pix
Si XIV	2.4	2.2	2.1	2.1	2.5	2.4	2.3	2.5
Si XIII	8.7	8.5	8.4	8.4	8.7	8.9	8.7	8.7
Mg XII	6.8	6.7	6.5	6.5	6.0	6.0	5.9	5.9
Mg XI	12.7	12.2	12.0	12.0	12.4	12.5	12.4	12.4
Ne X + Fe XVII	22.3	21.7	21.0	21.1	22.4	22.0	21.4	21.5
Fe XVII	75.8	75.6	71.0	71.0	78.1	77.2	74.5	74.3
O VIII	31.4	33.4	30.9	30.9	35.5	35.8	34.4	34.3
O VII	13.8	13.9	12.7	12.6	15.7	14.4	13.9	13.9
N VII	6.0	6.0	6.1	6.0	8.0	7.6	6.9	7.0

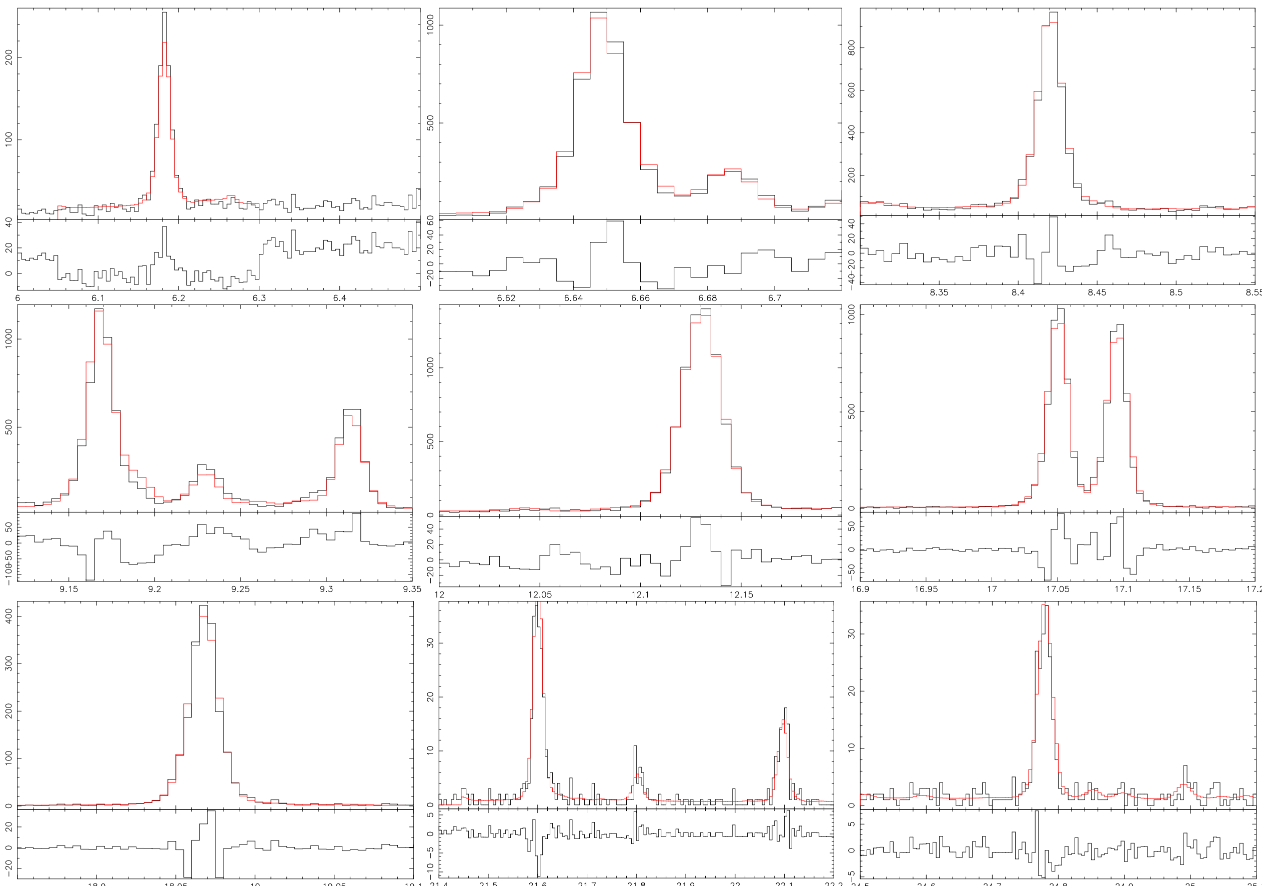

Figure 3: MEG $+1^{st}$ order: the results of line profile fitting with the thermal APED model on the merged Capella spectra. (Top panel) wavelength vs. total counts; (bottom panel) wavelength vs. residual in counts.

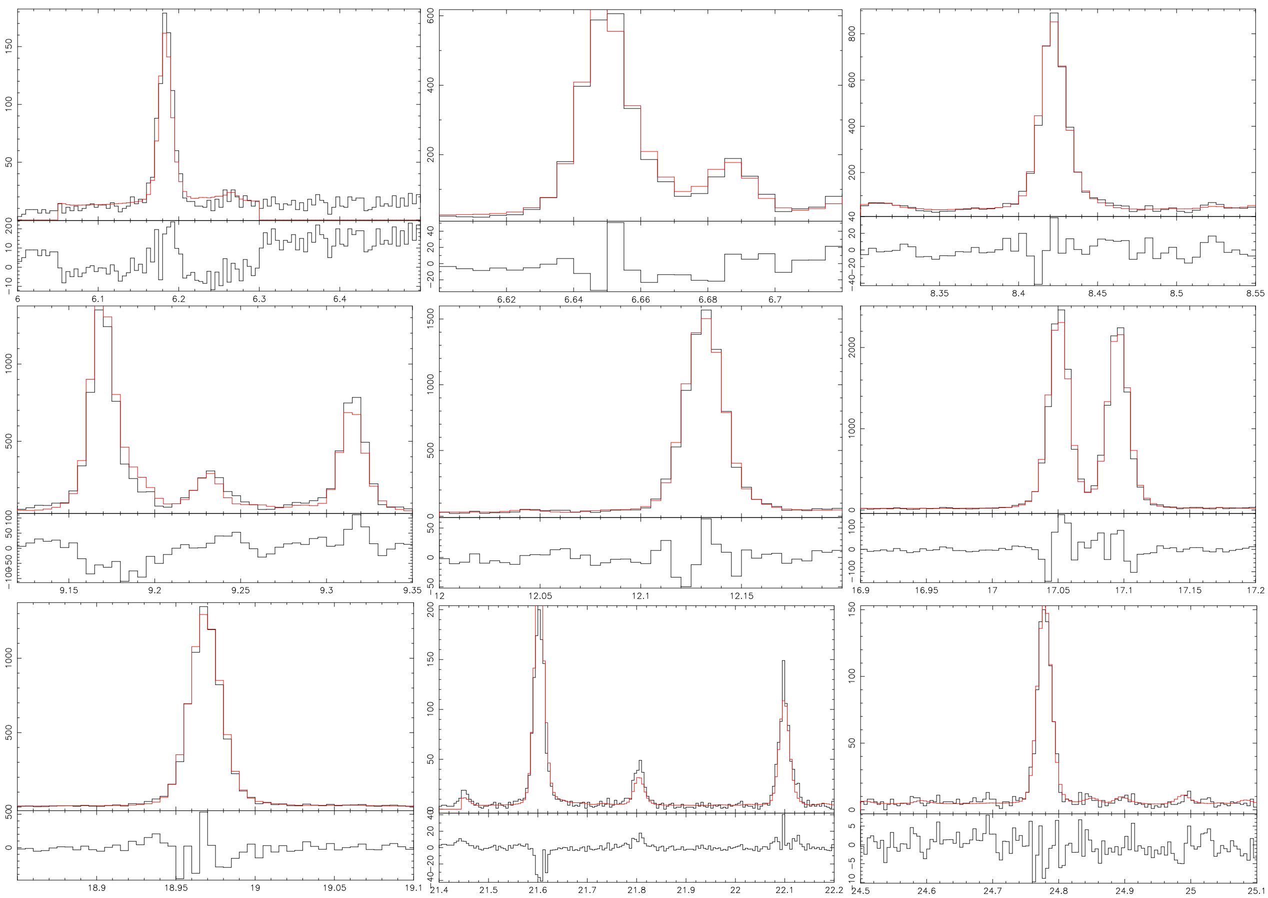

Figure 4: MEG -1^{st} order: the results of line profile fitting with the thermal APED model on the merged Capella spectra. (Top panel) wavelength vs. total counts; (bottom panel) wavelength vs. residual in counts.